New Open-Framework Ammonium and Amine Cadmium Zirconium Oxalates with Helical Structures

Erwann Jeanneau, Nathalie Audebrand, and Daniel Louër*

Laboratoire de Chimie du Solide et Inorganique Moléculaire (UMR 6511 CNRS), Institut de Chimie, Université de Rennes I, Avenue du Général Leclerc, 35042 Rennes Cedex, France

Received August 7, 2001. Revised Manuscript Received November 22, 2001

Two new open-framework cadmium zirconium oxalates containing ammonium or ethylenediamine have been prepared from precipitation methods at room pressure. The crystal data of these oxalates are as follows: **I**, $2[NH_4]^+[CdZr(C_2O_4)_4]^{2-}\cdot 3.9H_2O$, trigonal, space group $P6_422$ (no. 181), $a = 9.061(5)$ Å, $c = 23.394(5)$ Å, $V = 1663(1)$ Å^3, $Z = 3$, $R_1 = 0.03$; **II**, $[C_2N_2H_{10}]^{2+}[CdZr(C_2O_4)_4]^{2-}\cdot 4.4H_2O$, trigonal, space group $P3_112$ (no. 151), $a = 9.105(5)$ Å, $c = 23.656(5)$ Å, $V = 1698(1)$ Å^3, $Z = 3$, $R_1 = 0.04$. The two structures are built from MO_8 (M = Cd, Zr) distorted antiprisms connected by oxalate groups to give rise to chains based on the sequence ...−Cd−oxalate−Zr−oxalate−... that display a helical wire arrangement. Each helix is connected to six neighboring ones to form an anionic three-dimensional framework $[CdZr(C_2O_4)_4]^{2-}$ balanced by the cations NH_4^+ or $[NH_3-(CH_2)_2-NH_3]^{2+}$ located in tunnels parallel to the *c* axis that also contain water molecules. The apertures have hexagonal and square cross sections of ∼5.7 Å and ellipsoidal cross sections of 5.7 × 12 Å. There is extensive hydrogen bonding among the ammonium and amine groups, water molecules, and framework. The thermal decomposition of the two compounds into cadmium and zirconium oxides is described.

1. Introduction

Open-framework metal-oxalate-based compounds have received much attention in recent years, with the aim of discovering new types of porous solids (see, for example, ref 1). Additionally, the structure topology is often favorable to dynamic properties as a result of the presence of weakly bonded zeolitic water molecules located inside the voids of the structures.[2] Representative recent examples have been reported in which hydrothermal syntheses in the presence of structure-directing organic entities, such as amines,[3−5] are used, but the traditional precipitation of solutions at ambient pressure has also revealed some potentialities in the formation of such phases.[6,7] There is also an interest in the formation of oxalates with two metals for their ability to produce nanocrystalline mixed oxides from thermal decomposition. Typical examples are $BaTiO_3$ and $PbZrO_3$ obtained from barium titanyl oxalate hydrate[8] and lead zirconium oxalate hydrate,[9] respectively. Among the recently reported mixed oxalates are various well-characterized phases with metals having 8-fold coordination, e.g., $YK(C_2O_4)_2\cdot 4H_2O$[2]; $Pb_2Zr(C_2O_4)_4\cdot nH_2O$[9]; and, more recently, $Cd_2Zr(C_2O_4)_4\cdot nH_2O$.[10] In these structures, the concept of building units, discussed extensively in recent times (see, for example, ref 11), seems to be an approach to consider in this family of phases to conceive new compounds. The basic units are polyhedra formed by the metals with 8-fold coordination, such as ZrO_8 and CdO_8 in $Cd_2Zr(C_2O_4)_4\cdot nH_2O$, which exhibits a nanoporous topology related to the $YK(C_2O_4)_2\cdot 4H_2O$ structure type. The building units are linked through the oxalate groups. It has been anticipated that the formation of new structural arrangements from solution routes could be further extended by the addition in the synthesis stage of new elements or building units, which could then act as agents modifying existing structural arrangements. This is the driving idea that has been applied here for conceiving novel structural frameworks in the family of cadmium zirconium oxalates. The additional groups considered in the present study are ammonium and amine entities. This study deals with the nonhydrothermal synthesis, the crystal structure determination, and the thermal behavior of two new nanoporous cadmium zirconium oxalates.

2. Experimental Section

2.1. Preparation and Preliminary Characterization. Crystals of cadmium zirconium ammonium oxalate CdZr-

* Author to whom correspondence should be addressed. E-mail address: Daniel.Louer@univ-rennes1.fr. Fax: (33) 2 99 38 34 87.

(1) Rao, C. N. R.; Natarajan, S.; Choudhury, A.; Neeraj, S.; Vaidhyanathan, R. *Acta Crystallogr.* **2001**, *B57*, 1−12.
(2) Bataille, T.; Auffrédic, J.-P.; Louër, D. *Chem. Mater.* **1999**, *11*, 1559−1567.
(3) Natarajan, S.; Vaidhyanathan, R.; Rao, C. N. R.; Ayyappan, S.; Cheetham, A. K. *Chem. Mater.* **1999**, *11*, 1633−1639.
(4) Vaidhyanathan, R.; Natarajan, S.; Cheetham, A. K.; Rao, C. N. R. *Chem. Mater.* **1999**, *11*, 3636−3642.
(5) Prasad, P. A.; Neeraj, S.; Natarajan, S.; Rao, C. N. R. *Chem. Commun.* **2000**, 1251−1252.
(6) Audebrand, N.; Vaillant, M.-L.; Auffrédic, J.-P.; Louër, D. *Solid State Sci.* **2001**, *3*, 483−494.
(7) Vaidhyanathan, R.; Natarajan, S.; Rao, C. N. R. *J. Chem. Soc., Dalton Trans.* **2001**, 699−706.
(8) Louër, M.; Louër, D.; Gotor, F. J.; Criado, J. M. *J. Solid State Chem.* **1991**, *92*, 565−572.
(9) Boudaren, C.; Auffrédic, J.-P.; Louër, M.; Louër, D. *Chem. Mater.* **2000**, *12*, 2324−2333.
(10) Jeanneau, E.; Audebrand, N.; Auffrédic, J.-P.; Louër, D. *J. Mater. Chem.* **2001**, *11*, 2545−2552.
(11) Férey, G. *J. Solid State Chem.* **2000**, *152*, 37−48.

10.1021/cm0112136 CCC: $22.00
Published on Web 03/01/2002

$(C_2O_4)_4(NH_4)_2 \cdot 3.9H_2O$ (**I**) and cadmium zirconium ethylenediamine oxalate $CdZr(C_2O_4)_4(C_2N_2H_{10}) \cdot 4.4H_2O$ (**II**) were obtained by soft chemistry routes. The compounds were synthesized from a mixture of 0.50 g of cadmium nitrate $Cd(NO_3)_2 \cdot 4H_2O$ (Merck) and 0.37 g of zirconium oxynitrate $ZrO(NO_3)_2 \cdot xH_2O$ from Alpha [whose correct formula is $Zr(OH)_2(NO_3)_2 \cdot (1 + x)H_2O$][12] in 50 mL of water. This solution was titrated by a 0.1 mol L^{-1} oxalic acid solution in excess until a white precipitate was formed. The solution was heated to 90 °C, and 2 mL of NH_4OH (**I**) or ethylenediamine $C_2N_2H_8$ (**II**) was added under stirring. Finally, a few milliliters of concentrated HNO_3 was added slowly until complete dissolution. The evaporation of the solution at room temperature led to the formation of bipyramidal transparent crystals for compound **I** (average size = 100 μm) and hexagonal-shaped plates (average size = 500 μm) for compound **II**. The crystals were then filtered, washed with deionized water and ethanol, and dried under air. Powder X-ray diffraction patterns of the powdered crystals, obtained with a Siemens D500 diffractometer (λ = 1.5406 Å) indicated that the products were pure new materials. It was subsequently verified that the powder data were indexed by the structural results reported in the present study. Thermogravimetric (TG) analysis was carried out with a Rigaku Thermoflex instrument. Temperature-dependent X-ray diffraction (TDXD) was performed under dynamic air with a powder diffractometer combining a curved position-sensitive detector (PSD) from INEL (CPS 120) and a high-temperature attachment from Rigaku. The detector was used in a semi-focusing arrangement by reflection (Cu $K\alpha_1$ radiation) as described elsewhere.[13] The chemical formulas were derived from energy dispersive spectrometry (Cd/Zr ratio = 1), performed with a JSM 6400 spectrometer equipped with an Oxford Link Isis analyzer, and from the crystal structure determination reported below. They correspond to the chemical compositions $CdZr(C_2O_4)_4(NH_4)_2 \cdot 3.9H_2O$ and $CdZr(C_2O_4)_4(C_2N_2H_{10}) \cdot 4.4H_2O$ for **I** and **II**, respectively. These results were confirmed by manganimetric titration of the oxalate content in crystals, from which the numbers of oxalate groups per formulas units 3.98 (**I**) and 4.04 (**II**) were derived. It should be noted, as shown from the thermogravimetric analysis reported below, that the amine compound is slightly air-sensitive at room temperature. Assuming the above formulas, the yields found for the two synthesis were 57% for **I** and 55% for **II**. The powder diffraction diagrams of the two compounds were recorded and did not indicate the presence of impurities. The images captured with a JEOL JSM-6301 F scanning electron microscope (SEM) showed pseudomorphs of the initial crystals, with cracks due to the sensitivity of the material to the electron beam (Figure 1). In addition, from a magnified image, an etching pattern on the surface of compound **I** could be observed (Figure 1), as the probable consequence of the use of concentrated nitric acid in the course of the synthesis. The particular geometry of such etching patterns is generally related to the crystalline structure and surface defects of the product.[14] No such feature was observed on the surface of the crystals of compound **II**, even though the experimental approach used was similar.

2.2. Single-Crystal Structure Determination. A suitable single crystal for each compound was carefully selected. Intensity data were collected on a four-circle Nonius KappaCCD diffractometer, using Mo Kα radiation (λ = 0.71073 Å), through the program COLLECT.[15] Lorentz-polarization correction, peak integration, and background determination were carried out with the program DENZO.[16] Frame scaling and unit-cell parameter refinement were performed with the program SCALEPACK.[16] Numerical absorption correction was performed by modeling the crystal faces using NUMABS.[17] Crystallographic data and details on data collection and refinement are listed in Table 1. Structure drawings were carried out with Diamond 2.1b.[18]

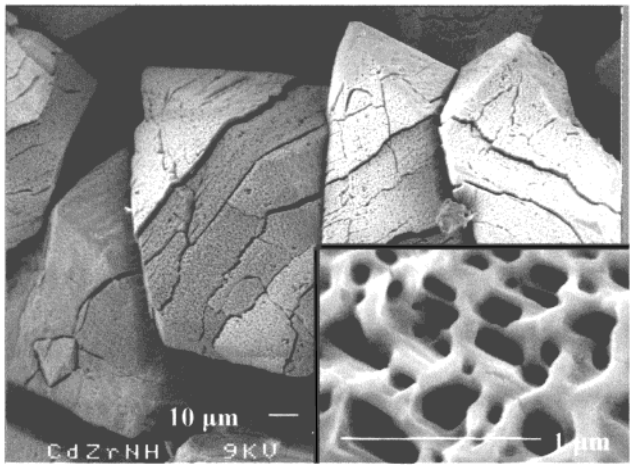

Figure 1. SEM micrograph displaying bipyramidal-shaped pseudomorphs of $CdZr(C_2O_4)(NH_4)_2 \cdot 3.9H_2O$, with cracks due to the sensitivity of the initial crystals to the electron beam. The closeup on the bottom right shows the typical etching pattern found on the surface of the crystals.

Both structures were solved using a hexagonal symmetry with space group $P6_422$ for compound **I** and space group $P3_112$ for compound **II**. Heavy atoms were located using direct methods by means of the program SIR97,[19] and the remaining non-H atoms were found from successive Fourier map analyses with SHELXL97.[20] Hydrogen atoms of the ammonium ion and water molecule in **I** were also found from Fourier analyses. For compound **II**, the hydrogen atoms of the amine group were placed by assuming a tetrahedral sp^3 hybridization for both the carbon and nitrogen atoms and were then refined using a "riding" mode, with the option included in SHELXL97.[20] Positions of the hydrogen atoms of water molecules were calculated, when possible, by means of the CALC-OH[21] program available in the WINGX software package[22] and then included in the refinement. As X-ray diffraction studies underestimate bonds involving hydrogen atoms, constraints were applied to keep them positioned in accordance with neutron diffraction studies.[23] N−H and O−H distances were thus constrained to be equal to 1.03(3) and 0.96(2) Å, respectively. Constraints on the H−H distances, 1.50(2) Å, were also included so that the H−O−H and H−N−H angles were close to the ideal tetrahedral angle. The last cycles of refinement included atomic positions for all atoms, anisotropic displacement parameters for all non-hydrogen atoms, and occupancy of the oxygen atoms from water molecules. The final refinement converged to site-occupancy factors for oxygen atoms of water molecules of 0.986(9) (**I**) and 0.500(1), 0.515(1), 0.546(2), and 0.64(1) (**II**), i.e., 3.94 ± 0.11 and 4.40 ± 0.24 water molecules per chemical formula. The final atomic coordinates and selected bond distances and angles are given in Tables 2 and 3 for **I**, and in Tables 4 and 5 for **II**.

(12) Bénard-Rocherullé, P.; Rius, J.; Louër, D. *J. Solid State Chem.* **1997**, *21*, 430−437.
(13) Plévert, J.; Auffrédic, J. P.; Louër, M.; Louër, D. *J. Mater. Sci.* **1989**, *24*, 1913−1918.
(14) Kachroo, S. K.; Bamzai, K. K.; Dhar, P. R.; Kotru, P. N.; Wanklyn, B. M. *Appl. Surf. Sci.* **2000**, *156*, 149−154.
(15) Nonius. *Kappa CCD Program Software*; Nonius BV: Delft, The Netherlands, 1998.
(16) Otwinowski, Z.; Minor, W. *Methods in Enzymology*; Carter, C.W., Sweet, R. M., Eds.; Academic Press: New York, 1997; Vol. 276, pp 307−326.
(17) Coppens, P. *Crystallographic Computing*; Ahmed, F. R., Hall, S. R., Huber, C. P., Eds.; Munksgaard Publishers: Copenhagen, 1970; pp 255−270.
(18) *Diamond 2.1b*; Crystal Impact: Bonn, Germany.
(19) Altomare, A.; Burla, M. C.; Camalli, M.; Cascarano, G.; Giacovazzo, C.; Guagliardi, A.; Moliterni, A. G. G.; Polidori, G.; Spagna, R. *J. Appl. Crystallogr.* **1999**, *32*, 115−119.
(20) Sheldrick, G. M. *SHELXL-97: Program for Crystal Structure Refinement*; University of Göttingen: Göttingen, Germany, 1997.
(21) Nardelli, M. *J. Appl. Crystallogr.* **1999**, *32*, 563−571.
(22) Farrugia, L. J. *J. Appl. Crystallogr.* **1999**, *32*, 837−838.
(23) Taylor, J. C.; Sabine, T. M. *Acta Crystallogr.* **1972**, *B28*, 3340−3351.

Table 1. Crystal Data and Structure Refinement Parameters of I, $CdZr(C_2O_4)_4(NH_4)_2 \cdot 3.9H_2O$, and II, $CdZr(C_2O_4)_4(C_2N_2H_{10}) \cdot 4.4H_2O$

	compound **I**	compound **II**
empirical formula	$CdZrO_{19.9}C_8N_2H_{15.8}$	$CdZrO_{20.4}C_{10}N_2H_{14.1}$
crystal system	trigonal	trigonal
space group	$P6_422$ (no. 181)	$P3_112$ (no. 151)
crystal size (mm)	0.170 × 0.155 × 0.125	0.260 × 0.220 × 0.080
a (Å)	9.061(5)	9.105(5)
c (Å)	23.394(5)	23.656(5)
V (Å^3)	1663(1)	1698(1)
Z	3	3
formula weight (g mol^{-1})	662.41	692.28
ρ_{calc} (g cm^{-3})	1.984	2.031
λ (Mo Kα) (Å)	0.71073	0.71073
μ (mm^{-1})	1.522	1.497
θ range (°)	2.60−34.96	2.58−34.93
index ranges	$-12 \le h \le 14$ $-12 \le k \le 14$ $-37 \le l \le 37$	$-13 \le h \le 14$ $-14 \le k \le 14$ $-29 \le l \le 38$
unique data	2451	4985
observed data [$I > 2\sigma(I)$]	1753	4589
refinement method	full-matrix least-squares on $\|F^2\|$	full-matrix least-squares on $\|F^2\|$
R_1 [$I > 2\sigma(I)$]	0.031	0.041
R_1 (all)	0.050	0.045
ωR_2 [$I > 2\sigma(I)$]	0.072	0.118
ωR_2 (all)	0.079	0.120
goodness of fit	1.08	1.22
no. of variables	89	180
no. of constraints	10	10
largest difference map peak and hole (e Å^{-3})	0.607 and −0.578	2.248 and −1.136

Table 2. Atomic Coordinates and Atomic Displacement Parameters (Å^2) in I, $CdZr(C_2O_4)_4(NH_4)_2 \cdot 3.9H_2O$

atom	x/a	y/b	z/c	U_{eq}[a]/U_{iso}
Cd	0.0000	0.5000	0.3333	0.01901(9)
Zr	0.5000	0.0000	0.5000	0.01547(9)
O1	0.9199(3)	0.2629(3)	0.38899(9)	0.0305(5)
O2	0.7344(3)	0.0832(2)	0.45216(8)	0.0267(4)
O3	0.5461(3)	0.2209(3)	0.44576(9)	0.0311(5)
O4	0.7388(3)	0.4354(3)	0.3913(1)	0.0350(5)
C1	0.7916(4)	0.2109(4)	0.4186(1)	0.0206(4)
C2	0.6854(3)	0.3011(4)	0.4176(1)	0.0232(4)
N1	0.0000	0.0000	0.5000	0.0317(9)
N2	0.0000	0.0000	0.3333	0.039(1)
Ow	0.7539(4)	−0.2435(4)	0.4162(1)	0.0594(8)
H1	0.8998(9)	−0.074(1)	0.4756(4)	0.05
H2	0.900(3)	−0.021(5)	0.691(1)	0.05
Hw1	0.643(3)	−0.256(5)	0.418(2)	0.05
Hw2	0.727(5)	−0.358(3)	0.420(2)	0.05

[a] $U_{eq} = (1/3)\sum_i\sum_j U_{ij} a_i^* a_j^* \mathbf{a}_i \cdot \mathbf{a}_j$.

Table 3. Selected Interatomic Distances (Å) and Bond Angles (°) for I, $CdZr(C_2O_4)_4(NH_4)_2 \cdot 3.9H_2O$

metal coordination[a]		bases of the antiprism	
Cd−O1, O1^{i,ii,iii}	2.297(2)	O1−O4	2.775(3)
Cd−O4, O4^{i,ii,iii}	2.530(2)	O1−O4^{iii}	2.930(3)
		O4−O1−O4^{iii}	96.89(9)
		O1−O4−O1^{iii}	83.07(9)
Zr−O2^{iii,iv,v,vi}	2.174(2)	O2^{v}−O3^{v}	2.572(3)
Zr−O3^{iii,iv,v,vi}	2.228(2)	O2^{iv}−O3^{v}	2.660(3)
		O3^{iv}−O2^{v}−O3^{v}	88.7(1)
		O2^{v}−O3^{v}−O2^{iv}	90.94(9)
oxalate anion			
C1−C2	1.542(3)	O1−C1−C2	120.7(2)
C1−O1	1.227(3)	O2−C1−C2	114.3(2)
C1−O2	1.275(3)	O3−C2−C1	113.0(2)
C2−O3	1.279(3)	O4−C2−C1	119.5(3)
C2−O4	1.227(3)	O1−C1−O2	125.0(2)
		O3−C2−O4	127.5(2)
organic moiety NH_4^+			
N1−H1, H1^{vii,viii,ix}	0.997(5)	H1−N1−H1^{vii}	110.97(5)
		H1−N1−H1^{viii}	103.56(2)
		H1−N1−H1^{ix}	114.06(2)
		H1^{vii}−N1−H1^{viii}	114.06(2)
		H1^{vii}−N1−H1^{ix}	103.56(2)
		H1^{viii}−N1−H1^{ix}	110.97(6)
N2−H2^{x,xi,xii,xiii}	1.005(3)	H2^{x}−N2−H2^{xi}	108.31(2)
		H2^{x}−N2−H2^{xii}	110.06(5)
		H2^{x}−N2−H2^{xiii}	110.04(2)
		H2^{xi}−N2−H2^{xii}	110.04(2)
		H2^{xi}−N2−H2^{xiii}	110.06(5)
		H2^{xii}−N2−H2^{xiii}	108.31(2)

[a] Symmetry codes: (i) $2 - x, 1 - x + y, {}^2/_3 - z$; (ii) $x, x - y, {}^2/_3 - z$; (iii) $2 - x, 1 - y, z$; (iv) $1 + x - y, 1 - y, 1 - z$; (v) $2 - x + y, 1 + y, 1 - z$; (vi) $1 + x, 1 + y, z$; (vii) $2 - x + y, y, 1 - z$; (viii) $2 - x, -y, z$; (ix) $x - y, -y, 1 - z$; (x) $-1 + x - y, -2 + x, -{}^1/_3 + z$; (xi) $3 - x + y, 2 - x, -{}^1/_3 + z$; (xii) $-1 + x - y, -y, 1 - z$; (xiii) $3 - x + y, y, 1 - z$.

3. Results

3.1. Description of the Structures. The two compounds exhibit similar three-dimensional arrangements of cadmium and zirconium polyhedra linked through oxalate groups. Both coordination polyhedra of the zirconium (Figure 2a) and cadmium (Figure 2b) atoms can be described as distorted square antiprisms similar to those found, for example, in $Pb_2Zr(C_2O_4)_4 \cdot nH_2O$.[9] The Zr−O distances are 2.174(2) and 2.228(2) Å and range from 2.180(3) to 2.258(3) Å for compounds **I** and **II**, respectively. The mean Zr−O distances (2.201 and 2.219 Å) agree with the theoretical value, 2.184 Å, found with the bond valence method using the program VALENCE.[24] The standard mean deviations from planarity of the zirconium antiprism bases equal 0.075 and 0.048 Å in compounds **I** and **II,** respectively. Moreover, the mean square planes of the zirconium polyhedra are strictly parallel for **I**, whereas they make an angle of 0.57° for **II**. The cadmium atom is also surrounded by eight oxygen atoms, forming a square antiprism with

(24) Brown, I. D. *J. Appl. Crystallogr.* **1996**, *29*, 479−480.

Table 4. Atomic Coordinates and Atomic Displacement Parameters (Å²) in II, $CdZr(C_2O_4)_4(C_2N_2H_{10})\cdot 4.4H_2O$

atom	*x*/*a*	*y*/*b*	*z*/*c*	U_{eq}[a]/U_{iso}
Cd	0.81331(2)	0.18669(2)	0.3333	0.02098(9)
Zr	0.29743(5)	0.14872(3)	0.5000	0.0157(1)
O1	0.5247(4)	0.3363(4)	0.4494(1)	0.0298(6)
O2	0.7346(5)	0.3669(4)	0.3921(2)	0.0351(7)
O3	0.5682(4)	0.0212(4)	0.3829(1)	0.0277(6)
O4	0.3851(4)	0.0108(4)	0.4476(1)	0.0251(5)
O5	0.0390(4)	0.3193(4)	0.3932(1)	0.0273(6)
O6	0.2123(4)	0.3045(4)	0.4556(1)	0.0265(6)
O7	0.8720(4)	−0.0294(4)	0.3876(2)	0.0346(7)
O8	0.0736(4)	−0.0205(4)	0.4458(1)	0.0290(6)
C1	0.6013(5)	0.2827(5)	0.4186(2)	0.0231(7)
C2	0.5139(5)	0.0891(5)	0.4152(2)	0.0208(6)
C3	0.0882(5)	0.2382(5)	0.4219(2)	0.0215(6)
C4	−0.0004(5)	0.0453(5)	0.417(2)	0.0224(6)
C	0.3686(7)	−0.4439(7)	0.3045(2)	0.041(1)
N	0.3301(6)	0.6731(6)	0.0664(2)	0.0407(9)
Ow1	0.8314(7)	−0.3258(6)	0.3364(2)	0.0159(8)
Ow2	0.1873(3)	−0.1873(3)	0.3333	0.046(1)
Ow3	0.2330(5)	−0.534(1)	0.1667	0.067(2)
Ow4	0.881(1)	0.2182(9)	0.1568(2)	0.047(2)
H1C	0.4431	−0.4758	0.2857	0.049
H2C	0.2602	−0.5463	0.3102	0.049
H1N	0.3284(6)	0.783(2)	0.0712(2)	0.061
H2N	0.442(2)	0.6982(7)	0.0488(3)	0.061
H3N	0.3168(6)	0.618(1)	0.1049(6)	0.061
H1w1	0.738(8)	−0.318(2)	0.332(6)	0.05
H2w1	0.929(8)	−0.224(8)	0.328(6)	0.05
Hw2	0.307(2)	−0.142(3)	0.331(6)	0.05
Hw3	0.281(2)	−0.607(3)	0.169(6)	0.05

[a] $U_{eq} = (1/3)\sum_i\sum_j U_{ij} a_i^* a_j^* \mathbf{a}_i \cdot \mathbf{a}_j$.

Table 5. Selected Interatomic Distances (Å) and Bond Angles (°) for II, $CdZr(C_2O_4)_4(C_2N_2H_{10})\cdot 4.4H_2O$

metal coordination[a]		bases of the antiprism	
Cd−O2, O2^{i}	2.513(4)	O2−O3	2.735(5)
Cd−O3, O3^{i}	2.293(3)	O3−O7	3.024(5)
Cd−O5, O5^{i}	2.281(3)	O7−O5	2.753(5)
Cd−O7, O7^{i}	2.618(4)	O5−O2	3.012(5)
		O2−O3−O7	98.6(1)
		O3−O7−O5	81.1(1)
		O7−O5−O2	98.5(1)
		O5−O2−O3	81.7(1)
Zr−O1, O1^{ii}	2.258(3)	O1−O4	2.576(4)
Zr−O4, O4^{ii}	2.180(3)	O4−O8	2.706(5)
Zr−O6, O6^{ii}	2.195(3)	O8−O6	2.582(4)
Zr−O8, O8^{ii}	2.243(3)	O6−O1	2.716(5)
		O1−O4−O8	90.6(1)
		O4−O8−O6	89.5(1)
		O8−O6−O1	90.2(1)
		O6−O1−O4	89.4(1)
oxalate anions			
C1−C2	1.531(5)	O1−C1−C2	113.7(3)
C1−O1	1.263(5)	O2−C1−C2	118.6(3)
C1−O2	1.234(5)	O3−C2−C1	119.9(3)
C2−O3	1.232(4)	O4−C2−C1	114.7(3)
C2−O4	1.279(4)	O1−C1−O2	127.7(3)
		O3−C2−O4	125.4(3)
C3−C4^{iii}	1.527(5)	O5−C3−C4^{iii}	120.4(3)
C3−O5	1.240(5)	O6^{iii}−C3−C4^{iii}	115.3(3)
C3−O6^{iii}	1.263(5)	O7−C4^{iii}−C3	119.1(4)
C4^{iii} −O7	1.231(5)	O8−C4^{iii}−C3	113.4(3)
C4^{iii} −O8^{iii}	1.293(5)	O5−C3−O6^{iii}	124.4(4)
		O7−C4^{iii}−O8^{iii}	127.5(4)
organic moiety $[NH_3-(CH_2)_2-NH_3]^{2+}$			
C−C^{iv}	1.53(1)	N^{v}−C−C^{iv}	114.0(4)
C−N^{v}	1.493(6)	C^{iv}−C−H1C, H2C	108.7
		H1C−C−H2C	107.6

[a] Symmetry codes: (i) $1-y, 1-x, 2/3-z$; (ii) $x, x-y, 1-z$; (iii) $1+x, y, z$; (iv) $1-y, 1-x, 1/3+z$; (v) $1-x+y, y-1, 1/3-z$.

Cd−O distances of 2.297(2) and 2.530(2) Å for compound **I** and Cd−O distances ranging from 2.281(3) to 2.618(4) Å for **II**. The mean Cd−O distances (2.414 and 2.426 Å) agree with the mean theoretical value, 2.414 Å, found by the bond valence method. Four of the eight Cd−O distances are longer than expected, whereas the remaining four are shorter. The bases have mean standard deviations from planarity of 0.028 Å in **I** and 0.022 Å in **II**. The two square planes of the cadmium polyhedra are strictly parallel in the case of compound **I**, whereas they make an angle of 0.62° in compound **II**.

Compound **I** contains only one oxalate group, whereas compound **II** has two crystallographically distinct oxalate moieties. The distances and angles for the different

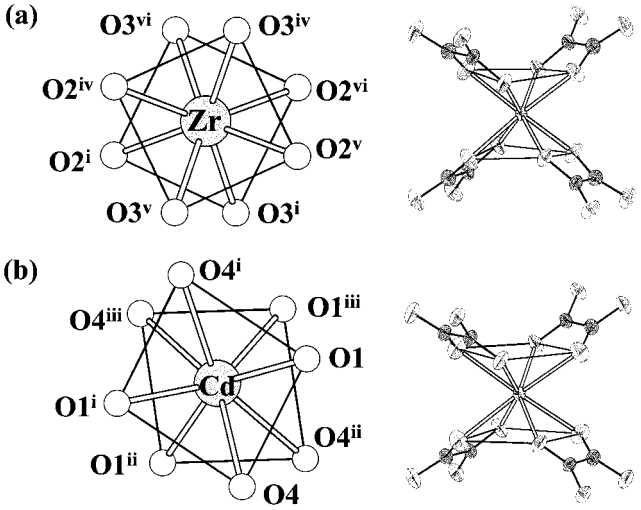

Figure 2. Coordination polyhedra of the (a) zirconium and (b) cadmium atoms in $CdZr(C_2O_4)(NH_4)_2\cdot 3.9H_2O$. The right-hand structures show the polyhedra with atomic-displacement ellipsoids plotted at the 50% probability level.

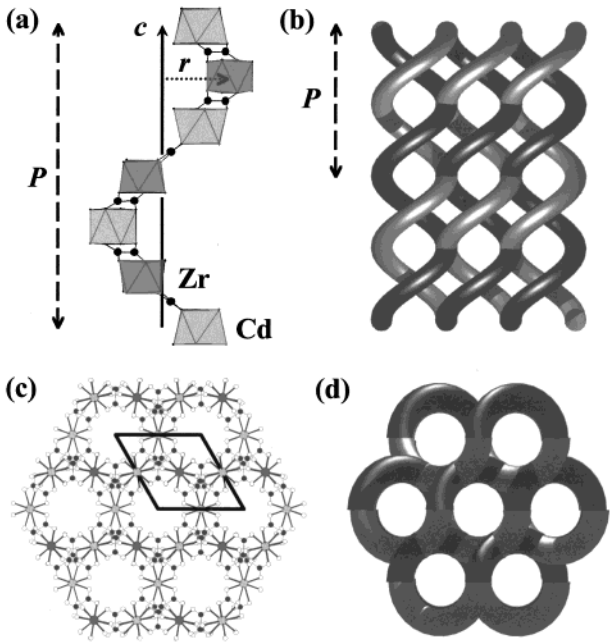

Figure 3. Helical representation of the anionic framework $[CdZr(C_2O_4)_4]^{2-}$ with (a) the drawing of one metal−oxalate helical-shaped chain, (b) a sketch of helix interconnections viewed along the *a* axis, and (c) a projection of the structure along the *c* axis together with (d) a sketch displaying the cross section of the tunnels parallel to *c*. The helix parameters are (**I**) $P = 23.394(5)$ Å, $r = 4.5315(5)$ Å and (**II**) $P = 23.656(5)$ Å, $r = 4.553(5)$ Å.

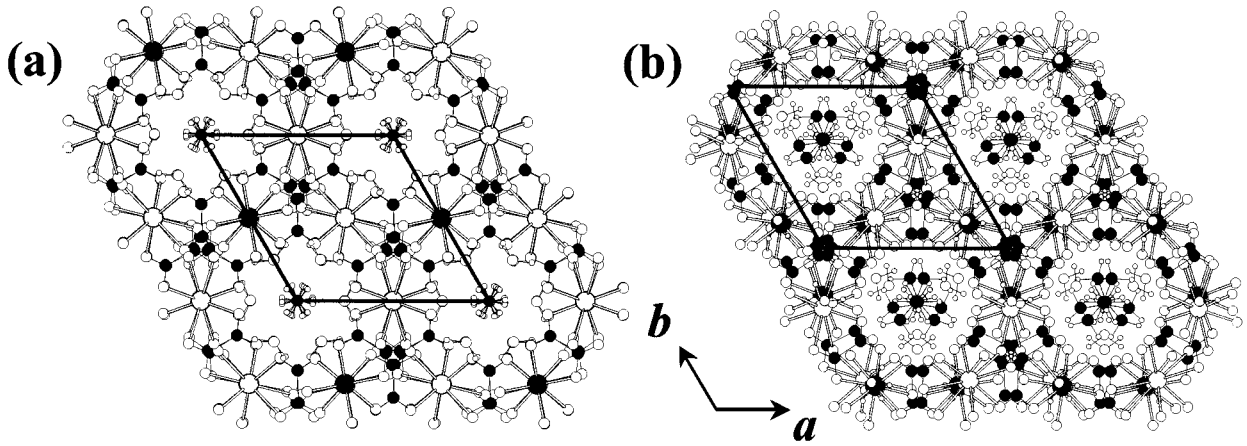

Figure 4. Projection of the structures along [001] of (a) $CdZr(C_2O_4)(NH_4)_2 \cdot 3.9H_2O$ and (b) $CdZr(C_2O_4)(C_2N_2H_{10}) \cdot 4.4H_2O$. Large light gray circles, Cd; large dark gray circles, Zr; small dark gray circles, N; small black circles, C; small white circles, O; smallest white circles, H.

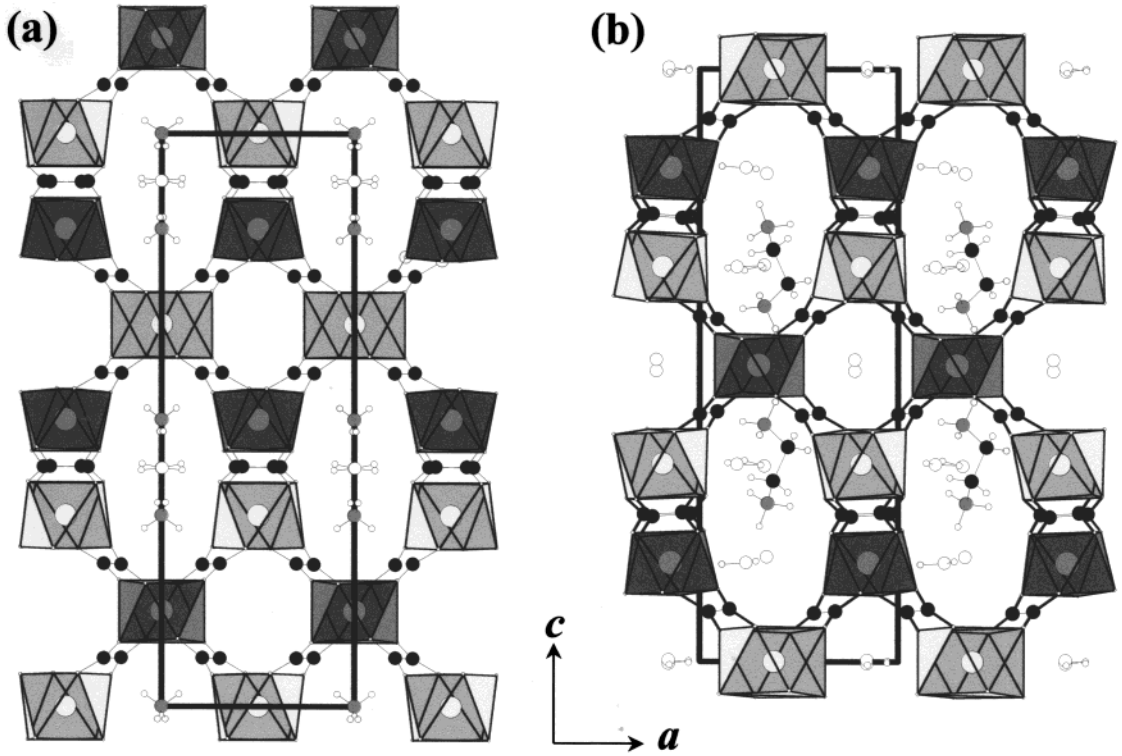

Figure 5. Projection of the structures along [010] of (a) $CdZr(C_2O_4)_4(NH_4)_2 \cdot 3.9H_2O$ and (b) $CdZr(C_2O_4)_4(C_2N_2H_{10}) \cdot 4.4H_2O$. Large light gray circles, Cd; large dark gray circles, Zr; small dark gray circles, N; small black circles, C; small white circles, O; smallest white circles, H.

oxalate groups are listed in Tables 3 (**I**) and 5 (**II**). They are in good agreement with the mean values reported by Hahn[25] for oxalate compounds, i.e., 1.24 and 1.55 Å, 117 and 126° for the C−O and C−C bond lengths and O−C−C and O−C−O angles, respectively. These oxalate groups are close to planarity, with mean atomic deviations from the least-squares planes of 0.059 Å (**I**) and 0.048 and 0.039 Å (**II**). The mean planes of the two oxalate groups in compound **II** make an angle of about 80° with respect to each other.

Both three-dimensional structures can be described as networks of right-handed metal−oxalate helical wires formed by connections through oxalate groups of the antiprisms described above (Figure 3). Figure 3a displays one helix, which consists of an alternation of metal atoms and oxalate groups, resulting in a Cd−oxalate−Zr−oxalate sequence. Such a helical wire can be described by two parameters (see Figure 3a): its period *P*, i.e., the axial distance between successive turns, which here equals the *c* unit-cell parameter, and its radius *r*, i.e., the distance between the helicoidal axis and a metal atom, corresponding here to *a*/2. A period of a helix consists of three cadmium polyhedra, three zirconium polyhedra, and six oxalate groups. The entire crystal structure can be reconstituted by applying a 180° rotation through the helix axis, which results in a double DNA-like helix, and then translating this double helix along the unit-cell axes (Figure 3b−d). Over one period, each helix is connected to six neighboring ones through its six constitutive metal polyhedra (Figure 3c and d).

(25) Hahn, T. *Z. Kristallogr.* **1957**, *109*, 438−466.

Table 6. Possible Hydrogen Bonds in I, $CdZr(C_2O_4)_4(NH_4)_2 \cdot 3.9H_2O$, and II, $CdZr(C_2O_4)_4(C_2N_2H_{10}) \cdot 4.4H_2O$

D−H···A[a]	*d*(D−H) (Å)	*d*(H···A) (Å)	∠D−H···A (°)	*d*(D···A) (Å)
		I		
N1−H1···O2	0.995(3)	2.674(5)	105(1)	3.071(6)
N1−H1···O2^{i}	0.955(3)	2.834(4)	95(1)	3.071(7)
N1−H1···Ow	0.955(3)	2.026(3)	166(1)	2.963(1)
N2−H2^{ii}···Ow	0.929(3)	2.042(5)	165(1)	2.95(1)
N2−H2^{ii}···O1^{iii}	0.929(3)	2.664(4)	110(3)	3.104(7)
N2−H2^{ii}···O1^{iv}	0.929(3)	2.909(5)	93(3)	3.103(7)
Ow−Hw1···O3^{v}	0.952(5)	1.99(6)	161(5)	2.907(6)
Ow−Hw1···O2	0.952(5)	2.85(8)	100(4)	3.168(6)
Ow−Hw2···O4^{vi}	0.946(5)	2.00(5)	158(3)	2.902(6)
Ow−Hw2···O4^{iv}	0.946(5)	2.86(7)	97(5)	3.116(6)
		II		
N−H1N···O5^{v}	0.984(1)	2.545(6)	162.65(5)	3.129(9)
N−H1N···O6^{vi}	0.984(1)	1.932(8)	117.99(4)	3.129(6)
N−H2N···O3^{vii}	0.985(3)	2.56(1)	103.18(4)	2.947(4)
N−H2N···Ow2^{vii}	0.985(3)	1.856(4)	161.99(3)	2.81(1)
N−H2N···O4^{vii}	0.985(3)	2.880(9)	99.40(4)	3.200(5)
N−H3N···Ow3^{viii}	0.983(1)	2.071(8)	138.49(2)	3.200(6)
N−H3N···O4^{vii}	0.983(1)	2.840(2)	102.50(3)	3.364(1)
C^{ix}−H1C^{ix}···Ow1^{x}	0.970(2)	3.054(8)	102.85(4)	3.403(4)
C^{ix}−H1C^{ix}···O1^{vi}	0.970(2)	2.767(6)	170.20(3)	3.727(8)
C^{ix}−H1C^{ix}···O6^{vi}	0.970(2)	2.93(1)	114.55(2)	3.45(1)
C^{ix}−H2C^{ix}···O3^{vii}	0.970(4)	2.557(3)	122.40(5)	3.184(6)
C^{ix}−H2C^{ix}···O5^{vii}	0.970(4)	2.65(1)	135.89(3)	3.41(1)
C^{ix}−H2C^{ix}···O7^{vii}	0.970(4)	2.74(1)	150.35(4)	3.61(1)
C^{ix}−H2C^{ix}···Ow1^{vii}	0.970(4)	2.968(3)	108.57(4)	3.403(4)
Ow1−H1w1···O7	0.929(4)	2.520(5)	98.31(3)	2.809(6)
Ow1−H1w1···Ow2^{xi}	0.929(4)	2.207(2)	123.76(5)	2.831(6)
Ow1−H1w1···Ow2^{x}	0.929(4)	2.798(7)	98.31(3)	2.809(6)
Ow1−H1w1···O4^{x}	0.929(4)	3.140(7)	91.18(2)	3.293(7)
Ow1−H2w1···O7	0.898(1)	2.632(9)	91.89(3)	2.809(6)
Ow1−H2w1···O5^{xii}	0.898(1)	3.153(6)	131.41(4)	3.808(7)
Ow1−H2w1···O6^{x}	0.898(1)	3.099(5)	113.87(2)	3.559(7)
Ow2−Hw2···O4	0.955(2)	3.003(7)	96.27(2)	3.25(1)
Ow2−Hw2···O3	0.955(2)	2.41(1)	143.36(4)	3.23(1)
Ow3−Hw3···Ow4^{xiii}	0.965(1)	1.906(2)	170.01(5)	2.861(4)
Ow3−Hw3···O3^{xiii}	0.965(1)	3.165(7)	103.84(2)	3.523(8)
Ow3−Hw3···O4^{xiii}	0.965(1)	3.04(1)	100.98(3)	3.36(1)

[a] Symmetry codes: (i) $x - y, -y, 1 - z$; (ii) $-1 + x - y, -2 + x, -^1/_3 + z$; (iii) $2 - x, -y, z$; (iv) $x, -1 + x - y, ^2/_3 - z$; (v) $1 - x + y, 2 - x, -^1/_3 + z$; (vi) $-x + y, 1 - x, -^1/_3 + z$; (vii) $1 - x + y, 1 - x, -^1/_3 + z$; (viii) $x, 1 + y, z$; (ix) $2 - x + y, 1 + y, ^1/_3 - z$; (x) $1 - y, -x, ^2/_3 - z$; (xi) $1 + x, y, z$; (xii) $1 - y, 1 - x, ^2/_3 - z$; (xiii) $1 - x + y, -1 + y, ^1/_3 - z$.

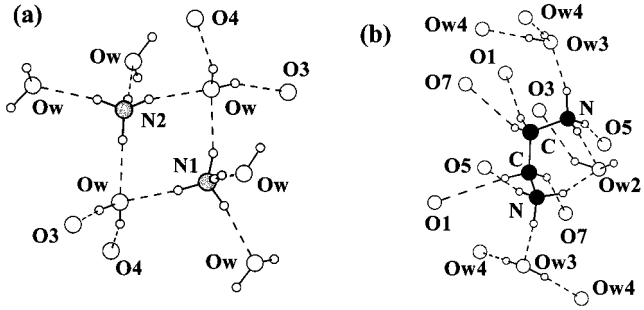

Figure 6. Strongest hydrogen bonds in (a) $CdZr(C_2O_4)_4(NH_4)_2 \cdot 3.9H_2O$ and (b) $CdZr(C_2O_4)_4(C_2N_2H_{10}) \cdot 4.4H_2O$.

Thus, each polyhedron belongs to two different metal−oxalate chains, rotated by 180° and translated by *a* with respect with each other. It should be noticed that, in compound **II**, the cadmium and zirconium polyhedra do not strictly superimpose as in **I**. This feature results in a slightly distorted framework (Figures 4b and 5b), probably due to the presence of the amine molecule, leading to a lowering in space group symmetry from $P6_4$-22 to $P3_112$.

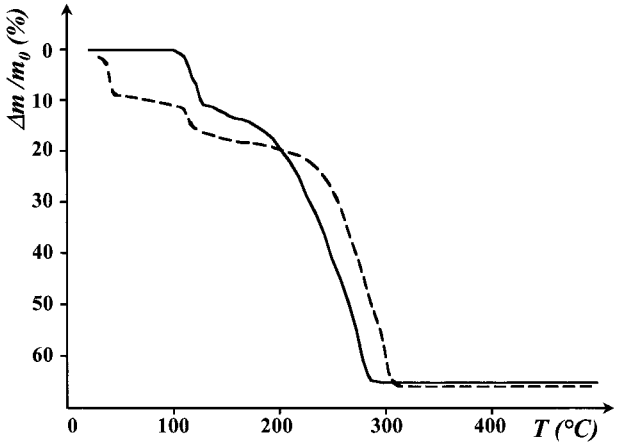

Figure 7. TG curves for $CdZr(C_2O_4)_4(NH_4)_2 \cdot 3.9H_2O$ (solid line) and $CdZr(C_2O_4)_4(C_2N_2H_{10}) \cdot 4.4H_2O$ (dotted line) under flowing air (5 °C h^{-1}).

The resulting charged open-framework $\{[CdZr(C_2O_4)_4]^{2-}\}_\infty$ constituted by this arrangement of helices displays tunnels along the three crystallographic axes and [110]. The tunnels along the *c* axis have a hexagonal cross section with a ∼5.7 Å diameter (Figures 3c and 4a and b). The projections along [110], *a*, or *b* display two kinds of tunnels: one with a square cross section of ∼5.7 Å and one with an ellipsoidal cross section of ∼5.7 × 12 Å (Figure 5a and b). Solvent-accessible voids were calculated by means of the program SOLV included in the software PLATON.[26] The total volumes available for guest water molecules and cations found by considering only the three-dimensional framework described above are 780 and 800 Å^3 for compounds **I** and **II,** respectively. These values correspond, for both structures, to approximately 47% of the total unit-cell volume.

Charge balance is achieved by the presence of guests in the tunnels. In the case of **I**, the $[CdZr(C_2O_4)_4]^{2-}$ framework is balanced by two NH_4^+ entities, whereas for **II**, ethylenediamine $[NH_3-(CH_2)_2-NH_3]^{2+}$ plays the role of counterion. The amine exhibits a staggered conformation with a N−C−C−N dihedral angle of 68.95°. These moieties lie along the helicoidal axis. The distance between two successive ammonium ions is *c*/6, and the distance is *c*/3 between two amines. In both compounds, the water molecules lie in the tunnels of the anionic framework. The distance between two water molecules lying in the tunnel along *c* is *c*/3, and the distance between water and amine molecules is *c*/6. There are numerous possible weak hydrogen bonds between the guest molecules and the host structure considering the criteria reported elsewhere (see, for example, ref 27). These hydrogen bonds are listed in Table 6, and the strongest ones are represented in Figure 6a (**I**) and b (**II**).

An alternative structural description could also be made using MC_8O_8 entities (M = Cd or Zr), instead of CdO_8 and ZrO_8 building units, in which the initial MO_8 polyhedra would incorporate the carbon atoms of the oxalate anions. The structure could thus be described

(26) Spek, A. L. *Acta Crystallogr.* **1990**, *A46*, C34.
(27) Desiraju, G. R.; Steiner, T. *The Weak Hydrogen Bond*; IUCr/OUP: Oxford, U.K., 2001.

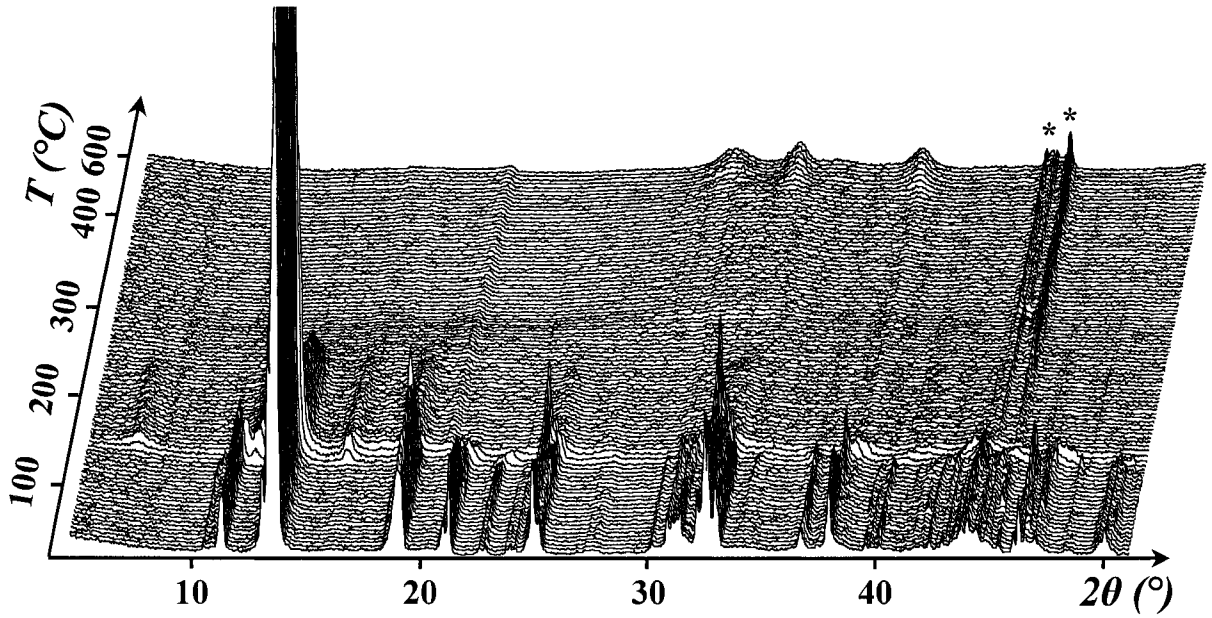

Figure 8. TDXD plot for $CdZr(C_2O_4)_4(NH_4)_2 \cdot 3.9H_2O$ under flowing air (heating rate = 5 °C h^{-1} in the range 20−400 °C, 15 °C h^{-1} in the range 400−600 °C; counting time = 3500 s/pattern). * indicates spurious diffraction lines due to the sample holder.

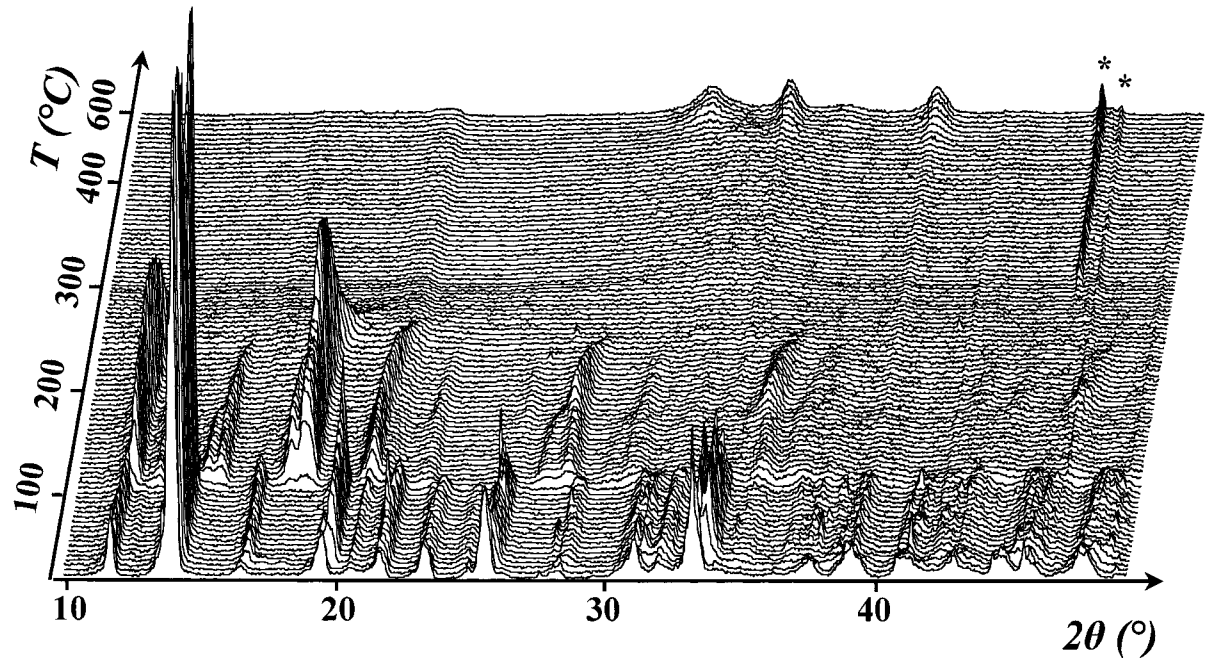

Figure 9. TDXD plot for $CdZr(C_2O_4)_4(C_2N_2H_{10}) \cdot 4.4H_2O$ under flowing air (heating rate = 5 °C h^{-1} in the range 20−400 °C, 15 °C h^{-1} in the range 400−600 °C; counting time = 3500 s/pattern). * indicates spurious diffraction lines due to the sample holder.

as a framework formed by edge-sharing MC_8O_8 building units.

3.2. Thermal Behaviors. The thermal decompositions of the two compounds were studied by thermogravimetric (TG) analyses (Figure 7) and temperature-dependent X-ray diffraction (TDXD) (Figures 8 and 9) from room temperature to 600 °C. From Figure 8, it can be seen that the decomposition of $CdZr(C_2O_4)_4(NH_4)_2 \cdot 3.9H_2O$ can be described as a three-step process. The precursor is stable up to ∼120 °C, where a new crystalline phase is formed, which is stable until ∼250 °C. From ∼280 °C, no diffraction lines are observed, and finally, very broad lines of nanocrystalline cubic CdO (33.0° 2θ, 38.3° 2θ) and tetragonal ZrO_2 (30.3° 2θ, 35.3° 2θ) appear at about ∼400 °C. However, the TG curve (Figure 7) displays an inflection point at ∼120 °C (observed weight loss of ∼6%). Because the TDXD plot (Figure 8) does not show any significant change until 120 °C, the framework of the structure remains unchanged, and thus, the weight loss can be attributed to the release of weakly bonded water molecules located in the tunnels. Consequently, the inflection point would correspond to the calculated formula $CdZr(C_2O_4)_4(NH_4)_2 \cdot 1.7H_2O$. After this inflection point, the weight loss is continuous until ∼290 °C. The chemical composition of the intermediate crystalline phase, observed between 120 and 280 °C in the TDXD plot, could not be determined because of the absence of any well-defined plateau in the TG curve. To characterize this phase, diffraction patterns were recorded at selected temper-

atures between 110 and 145 °C. The low resolution of the diffraction data ($\langle FWHM \rangle = \sim 0.2°\ 2\theta$) prevented the indexing of the patterns. However, it can be expected that the removal of the remaining water molecules and ammonium groups occurs in this temperature range, with the subsequent decomposition of the oxalate groups. For the last stage observed in the TG plot, the total weight loss (65%) is in agreement with the formation of cadmium and zirconium oxide mixture (calcd 62%), as verified from X-ray powder diffraction data.

The decomposition of $CdZr(C_2O_4)_4(C_2N_2H_{10})\cdot 4.4H_2O$ is more complicated. Indeed, the product starts with a progressive weight loss between ambient temperature and 35 °C (Figure 7). This feature can be explained by the departure of the less-bonded water molecules located in the tunnels (Figure 5). This phenomenon is accompanied by a slight shift of some lines toward higher angles (see, for example, the diffraction line at ~19.2° 2θ in Figure 9), corresponding to a light contraction of the structure framework. From 35 °C, the mass loss is due to the departure of the most-bonded water molecules, and the dehydration is completed at 110 °C, leading to the anhydrous compound $CdZr(C_2O_4)_4(C_2N_2H_{10})$ (weight loss of 11.2%, calcd 11.4%). However, apart from the slight line shift, no additional significant change is seen on the successive diffraction patterns until 110 °C, which means that the dehydration is not accompanied by a significant structural change. From the TDXD experiment (Figure 9), it can be seen that two successive intermediate phases are subsequently formed. The first one appears between 110 and 120 °C and transforms at ~180 °C, for which a weight loss of 18.3% is observed in the TG curve. This result could correspond to the departure of amine groups from the structure (calcd 20%), even though amine molecules are usually removed at higher temperatures.[28] Thus, it can be concluded that, as expected from the structure analysis, the interaction between the amines and the framework must be very weak. Indeed, the amine groups located inside the tunnels are initially stabilized by a hydrogen-bonding scheme involving the water molecules. It is clear that, after the departure of these water molecules, the hydrogen-bonding scheme is weakened, which favors the amine molecules to leave the structure at lower temperatures. The last intermediate crystalline phase seen in the TDXD plot decomposes between 250 and 280 °C. Over the temperature range where this phase is present, a continuous weight loss is observed (Figure 7). Because of the low quality of the data, no structural information on the two intermediate phases could be extracted from the study of powder patterns recorded at selected temperatures between 110 and 250 °C. As for the ammonium compound, an amorphous phase preceded the formation of nanocrystalline cubic CdO and tetragonal ZrO_2 oxides at ~400 °C. For the last stage observed in the TG plot, the total weight loss (66%) is in satisfactory agreement with the formation of a mixture of cubic cadmium oxide and tetragonal zirconium oxide (calcd 64%), as verified by the X-ray powder diffraction data. The presence of tetragonal ZrO_2 is in accordance with many studies in which the oxide is crystallized from an amorphous state.[29−31] However, it is worth noting that the final zirconium oxide polymorph obtained here differs, in both cases, from that observed in the thermal decomposition of the chemically related compound $Cd_2Zr(C_2O_4)\cdot nH_2O$, in which the formation of cubic cadmium-stabilized ZrO_2 was clearly pointed out.[10]

4. Concluding Remarks

The present study shows that new ternary (ammonium and amine) cadmium zirconium oxalates with open frameworks can be obtained through a simple synthesis route. These two compounds extend the family of cadmium zirconium oxalates, whose first member was the binary phase $Cd_2Zr(C_2O_4)_4\cdot nH_2O$[10] with the YK-$(C_2O_4)_2\cdot 4H_2O$ open-structure-type. The structure of all of these phases can be considered as formed from basic building units MO_8 (here M = Cd, Zr) linked through oxalate groups. The two new compounds exhibit a three-dimensional channel structure, with a charged framework $[CdZr(C_2O_4)_4]^{2-}$ built from interconnected helical chains that are balanced by cations located inside the tunnels. The entities inserted here in the tunnel are NH_4^+ in **I** and ethylenediamine $[NH_3\text{-}(CH_2)_2\text{−}NH_3]^{2+}$ in **II**, in addition to water molecules. An interesting feature of the new open frameworks is the presence of cations with different valences located in the channels. This opens up the possibility of synthesizing ternary cadmium zirconium oxalates of various amines or metals, e.g., monovalent or divalent metals possibly exhibiting interesting dynamical, substitution, and physical properties.

Acknowledgment. The authors are indebted to Dr. T. Roisnel and Mr. G. Marsolier for their technical assistance in diffraction data collection.

CM0112136

(28) Ayyappan, S.; Cheetham, A. K.; Natarajan, S.; Rao, C. N. R. *Chem. Mater.* **1998**, *10*, 3746−3755.

(29) Mamott, G. T.; Barnes, P.; Tarling, S. E.; Jones, S. L.; Norman, C. J. *Powder Diffr.* **1988**, *3*, 234−239.

(30) Bénard, P.; Auffrédic, J. P.; Louër, D. *Powder Diffr.* **1993**, *8*, 39−46.

(31) Srinivasan, R.; Hubbard, C. R., Cavin, O. B.; Davis, B. H. *Chem. Mater.* **1993**, *5*, 27−21.